Bioorganic & Medicinal Chemistry 18 (2010) 1806–1815

Contents lists available at ScienceDirect

Bioorganic & Medicinal Chemistry

journal homepage: www.elsevier.com/locate/bmc

# Design, synthesis, and biological evaluation of novel water-soluble triptolide derivatives: Antineoplastic activity against imatinib-resistant CML cells bearing T315I mutant Bcr-Abl

Fang Xu [a,b,†], Xianping Shi [b,†], Shichang Li [a], Jieshun Cui [a], Zhongzheng Lu [b], Yanli Jin [b], Yongcheng Lin [a], Jiyan Pang [a,*], Jingxuan Pan [b,*]

[a] School of Chemistry and Chemical Engineering, Sun Yat-Sen University, 135 Xingangxi Road, Guangzhou 510275, People's Republic of China
[b] Department of Pathophysiology, Zhongshan School of Medicine, Sun Yat-sen University, 74 Zhongshan Road II, Guangzhou 510089, People's Republic of China

ARTICLE INFO

*Article history:*
Received 13 December 2009
Revised 19 January 2010
Accepted 20 January 2010
Available online 25 January 2010

*Keywords:*
Triptolide
Derivatives
Synthesis
RNA polymerase
Inhibitor
Modeling
Tyrosine kinase inhibitors
Imatinib-resistance
CML

ABSTRACT

Imatinib (STI571) is the frontline targeted-therapeutic agent for patients with chronic myelogenous leukemia (CML). However, resistance to imatinib due to point mutations in Bcr-Abl kinase domain is an emerging problem. We recently reported that triptolide (compound **1**) could effectively kill CML cells including those harboring T315I mutant Bcr-Abl. In the present study, we designed a series of C-14 triptolide derivatives with C-14-hydroxyl substituted by different amine esters (**3**–**18**): **3**–**6** and **13** (by aliphatic chain amine esters); **7**–**9**, **11**, **12** and **15**–**18** (by alicyclic amine esters with different size), and **10** and **14** (by aralkylamine esters).The compounds were examined for their antineoplastic activity against CML cells (including KBM5-T315I cells) in terms of proliferation inhibition, apoptosis and signal transduction. Nude mouse xenograft model was also used to evaluate the in vivo activity. Compounds **2–9**, **11**–**14**, **17** and **18** exhibited a potent inhibitory activity against KBM5 and KBM5-T315I cells. This series of derivatives down-regulated Bcr-Abl mRNA. Compounds **4**, **5**, **8** and **9** were further examined for their impact on signaling and apoptosis with immunoblotting. Compound **5** was chosen for evaluation in a nude mouse xenograft model. The stereo-hindrance of C-14 group appeared to be responsible for the antitumor effect. The computational small molecule-protein docking analysis illustrated the possible interaction between compound **9** and RNA polymerase II. Our results suggest that this series of derivatives may be promising agents to overcome imatinib-resistance caused by the Bcr-Abl-T315I mutation.


## 1. Introduction

The cytoplasmic tyrosine kinase Bcr-Abl, the product of a fusion gene formed by a reciprocal chromosomal translocation t(9,22)(q34;q11), is found in approximately 95% patients with chronic myelogenous leukemia (CML) and 30% of adult patients with acute lymphoblastic leukemia.[1–3] The aberrant tyrosine kinase activity of this chimeric protein is responsible for malignant transformation by activating multiple signal transduction pathways.[4] Therefore, Bcr-Abl has been an important target for leukemia therapeutics.[5] Imatinib mesylate (STI571, Gleevec, Norvartis) was the first small molecule inhibitor approved by the US Food and Drug Administration. Imatinib effectively inhibits tyrosine kinase activity by occupying the ATP-binding pocket of Bcr-Abl and stabilizes the kinase in an inactive conformation, thus abrogating subsequent signal transduction.[6] Of newly diagnosed patients with chronic-phase CML, 82% showed complete cytogenetic response on treatment with imatinib over a median follow-up of 54 months.[7]

However, there are primary refractory disease and acquired resistance to imatinib, particularly in patients with advanced-phase disease.[5] Although several mechanisms have been proposed to explain acquired resistance to imatinib, mutation in the kinase domain of Bcr-Abl is believed to be the predominant mechanism.[8–12] Approximately 50 point mutations have been identified to be associated with clinical resistance to imatinib.[13] To overcome acquired resistance to imatinib, new tyrosine kinase inhibitors such as nilotinib, dasatinib and INNO-406 have been developed and are effective against all but the T315I mutation.[14–16] The prognosis for patients whose disease does not respond to imatinib, nilotinib and dasatinib is poor. Hence, novel strategies or compounds to overcome this challenging resistance are required, and, as demonstrated by recent reports,[17,18] lowering the expression of Bcr-Abl is a promising strategy.

*Tripterygium wilfordii* Hook. f., one of the traditional Chinese medicine, has been used for centuries to treat inflammation and

* Corresponding authors. Tel./fax: +86 20 87332788 (J. Pan).
*E-mail addresses:* panjx2@mail.sysu.edu.cn (J. Pan), or cespjy@mail.sysu.edu.cn (J. Pang).
† These authors contributed equally to this work.

0968-0896/$ - see front matter © 2010 Elsevier Ltd. All rights reserved.
doi:10.1016/j.bmc.2010.01.052

autoimmune diseases.[19–21] Among the many small molecules extracted and purified from this shrub-like vine, triptolide (compound **1**) (Fig. 1) is the key biologically active component that mediates immunosuppression and anti-inflammation.[22] Besides, triptolide possesses antitumor activities against a broad range of human cancer cells.[23–25] Recently, we and others have demonstrated that triptolide is an inhibitor of RNA polymerase I and II, causing global transcription inhibition.[26–29] Global transcriptional or translational inhibition would result in different degrees of decreases in protein levels among different proteins due to different degradation rates. We and others have demonstrated that triptolide at low nanomolar concentrations can effectively kill imatinib-resistant CML cells bearing T315I Bcr-Abl, hypereosinophilic leukemia cells bearing T674I PDGFRα, and mast leukemia cells bearing D816V KIT by inhibiting transcription of Bcr-Abl, PDGFRα and KIT, respectively.[26,27,29,30] Importantly, triptolide inhibits the growth of xenografted Bcr-Abl-T315I CML cells in nude mice,[30] and primary cells from CML patient with clinical resistance to imatinib.[29,30] These findings suggest that triptolide may be a promising agent in leukemia cells harboring mutant tyrosine kinase; however, its clinical development has been challenged by severe toxicity and water-insolubility.

Structure–activity relationship analysis in previous reports has demonstrated that the characteristic hydrogen-bonded C14 in triptolide is a key functional group for its antitumor effect.[23,31] Attempts to improve the solubility of **1** were documented previously.[31,32] For example, 14-succinyl triptolide sodium salt (PG490-88) is a prodrug that is converted to triptolide in serum and it retains all the toxicity of **1**.[32] Substituting C14-hydroxyl group of **1** with fluoride can keep the antitumor activity while lowering the side effects.[33] Nevertheless, little is known about the molecular interaction between the derivatives of **1** and the target, RNA polymerase II.

In this study, we designed a series of novel triptolide derivatives by substituting C-14-hydroxyl with different amine esters (**3**–**18**). The antitumor activity of these analogues was evaluated in imatinib-sensitive KBM5 cells and imatinib-resistant KBM5-T315I CML cells in vitro and in a nude mouse model. Computational docking analysis of these derivatives to RNA polymerase II was also conducted. Our results demonstrated that this series of novel C-14 substituted derivatives of triptolide are promising antitumor drug candidates to overcome the imatinib-resistance.

## 2. Chemistry

Cationic amine group can facilitate the contact between biomacromolecule and small molecules by electrostatic interactions. In most instances, a limited numbers of electrostatic interactions contribute to the binding energy of association. Hydrogen bonds and salt-bridges are believed to confer specificity to interactions due to their dependence on the precise location of participating atoms.[34,35] We hypothesized that the characteristic hydrogen-bonded C-14 in **1** substituted with amine groups may potently inhibit the growth of CML cells with Bcr-Abl-T315I mutation. We designed a series of C-14 triptolide derivatives with C-14-hydroxyl substituted by different amine esters (**3**–**18**): **3**–**6** and **13** (by aliphatic chain amine esters); **7**–**9**, **11**, **12** and **15**–**18** (by alicyclic amine esters with different size), and **10** and **14** (by aralkylamine esters) (Fig. 1). **14** was the combination of functional moieties of **1** and imatinib.

The synthetic approach used for the preparation of compounds **2–18** is outlined in Scheme 1. Chloroacetyl of **1** at 0 °C, gave **2** in

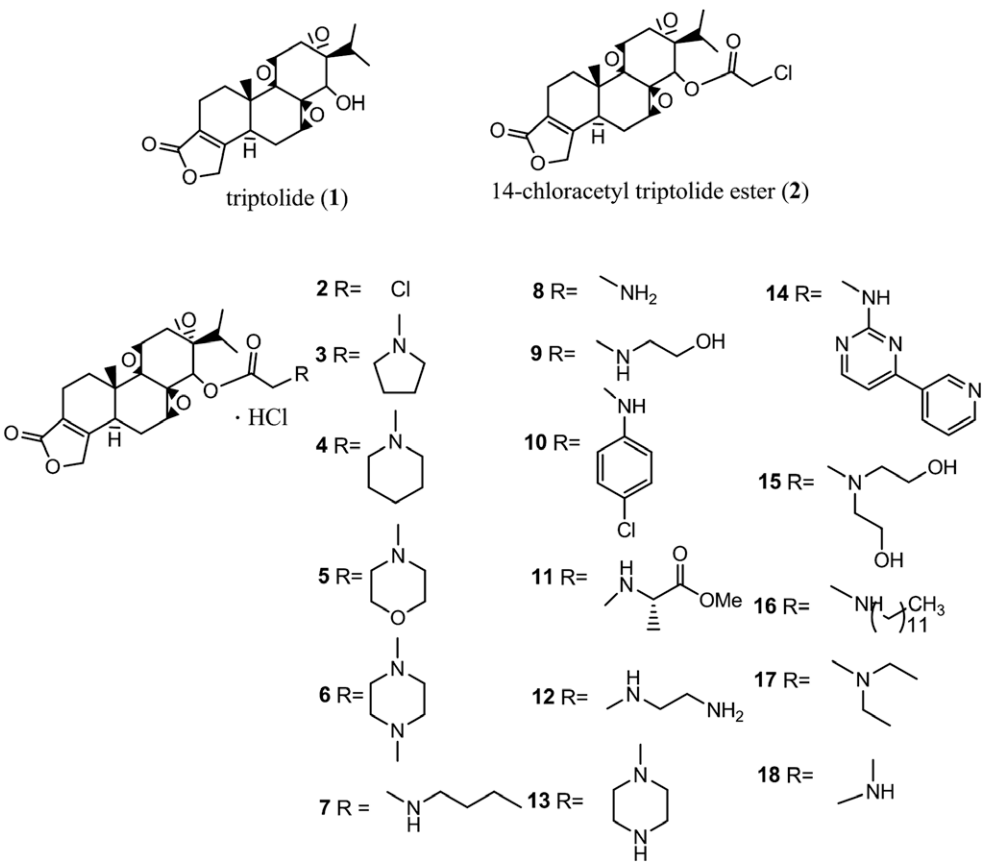


**Figure 1.** Structure of triptolide (compound **1**) and its derivatives (**2**–**18**).

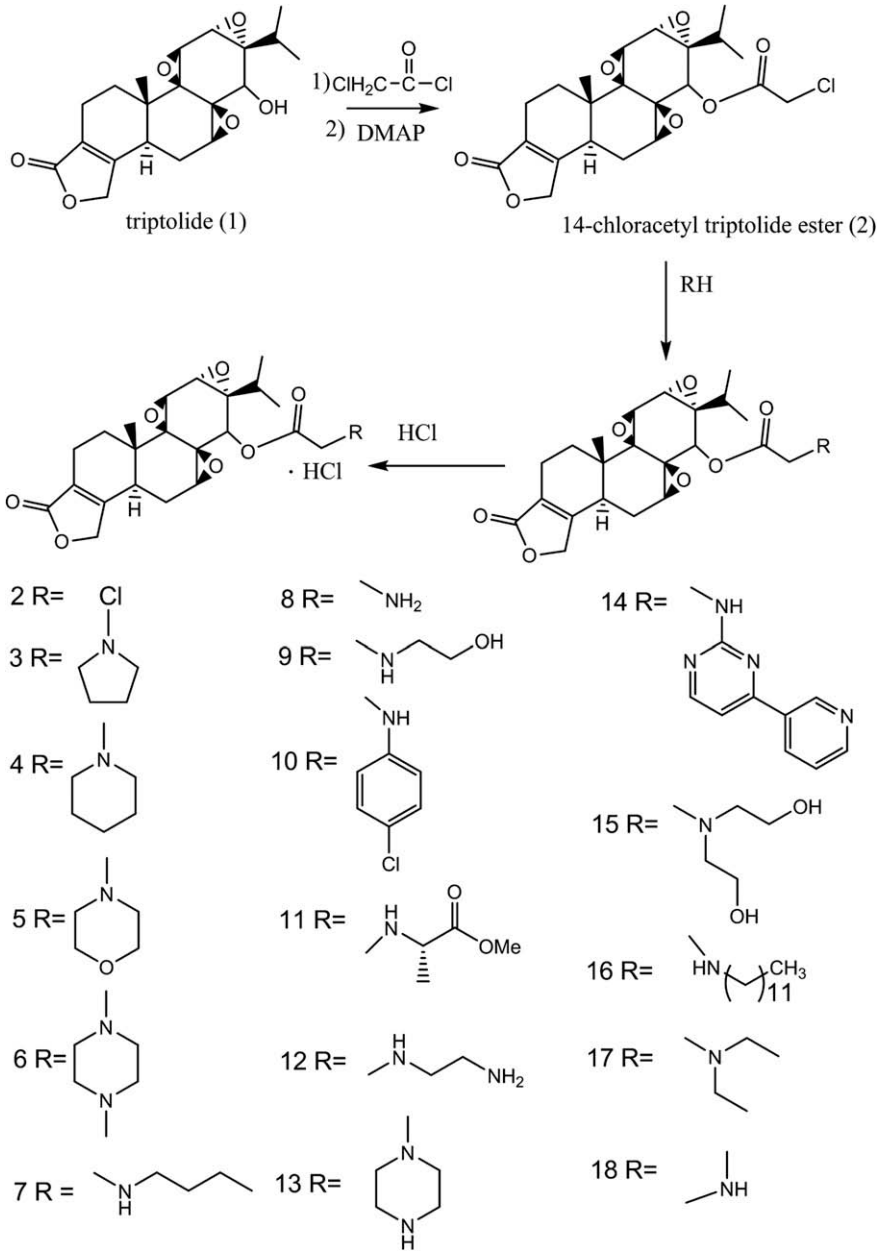


**Scheme 1.** Synthetic route for compounds **2**–**18**.

74.2% yield. Ammonolysis of **2** with different amines synthesized **3**–**18** in 55–90% yields. Compounds **2**–**18** were fully characterized by HRMS and NMR ($^1$H and $^{13}$C). They afforded HRMS spectra with the *m*/*z* values corresponding to $[M]^+$. Their NMR spectra were in full agreement with the given structures. The purity was judged from mass spectrometry, $^1$H NMR, and being single spots on TLC developed by different eluting solvents.

## 3. Results and discussion

### 3.1. Triptolide derivatives inhibits growth of imatinib-sensitive and -resistant CML cells

T315I in Bcr-Abl is a notorious point mutation eliciting resistance to imatinib. We recently found a KBM5 CML cell line harboring wild-type Bcr-Abl and a variant line harboring T315I Bcr-Abl (KBM5-T315I) with different sensitivities to imatinib; $IC_{50}$ values were 0.28 μM and 5.4 μM, respectively.[30,36] KBM5 and KBM5-T315I cells were incubated for 72 h with increasing concentrations of various derivatives of triptolide. Cell viability of both cell types was examined by the MTS assay, and $IC_{50}$ values were listed in Table 1. Representative dose–response curve were shown in Figure 2. Compounds **10**, **15** and **16** exhibited weak potency, while all the rest analogues including **14** exhibited potent inhibitory effect against both KBM5 and KBM5-T315I cells. We discovered that the bigger the substituted group was, the weaker the antitumor effect was (compared with **7** and **16**), and that different heteroatom might give different effects (compared **4**, **5** and **6**; **10** and **14**). To confirm the effect of triptolide derivatives on imatinib-resistant CML cells, we used an additional pair of murine myeloid cells 32D stably transfected with either wild-type or T315I Bcr-Abl. The data confirmed that imatinib-resistant 32D-T315I cells were also sensitive to the derivatives (**4**, **5**, **8** and **9**). The $IC_{50}$ values were listed in Table 2. Taken together, the results support that the stereo-hindrance of C-14 group is important for the antitumor effect of these triptolide derivatives.

**Table 1**
$IC_{50}$ values of derivatives of compound **1** based on 72-h incubation

| Compound | R | $IC_{50}$ (nM) | |
|---|---|---|---|
| | | KBM5 | KBM5-T315I |
| **1** | | 10.3 | 8.3 |
| **2** |  | 27.2 | 52.8 |
| **3** |  | 46.7 | 24.6 |
| **4** | 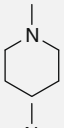 | 32.2 | 45.4 |
| **5** | 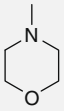 | 52.5 | 20.7 |
| **6** | 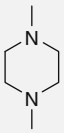 | 327.1 | 160.8 |
| **7** | 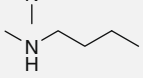 | 51.3 | 29.1 |
| **8** |  | 19.2 | 11.7 |
| **9** | 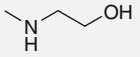 | 18.2 | 19.7 |
| **10** | 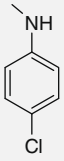 | 5020 | 734 |
| **11** | 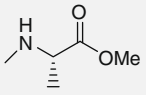 | 18.6 | 14.2 |
| **12** | 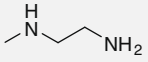 | 774 | 950 |
| **13** | 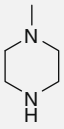 | 496 | 548 |
| **14** | 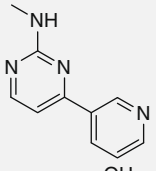 | 297 | 214.4 |
| **15** | 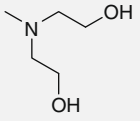 | 2800 | 1550 |
| **16** | 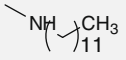 | 5420 | 1040 |
| **17** |  | 78 | 86 |
| **18** |  | 348 | 308 |

The effect of the derivatives (**4**, **5**, **8** and **9**) on normal cells was also determined. Normal fibroblasts [mouse embryonic fibroblasts (MEF) and normal human fibroblasts (NHFB)] were treated with increasing concentrations of the derivatives for 72 h, cell viability was assayed by MTS. The $IC_{50}$ values in MEF and NHFB cells ranged from 8800 to 11,500 nM) (Table 2), implying that there is a therapeutic window to use triptolide derivatives to treat CML.

### 3.2. Derivatives of triptolide inhibit RNA polymerase activity and induce apoptosis

We next examined whether the derivatives of **1**, like their parental compound triptolide, exerted their effect on the expression of Bcr-Abl which is the critical driving force for the transformation of CML cells. Based on $IC_{50}$ values, compounds **4**, **5**, **8**, or **9** were selected in such experiments. After 18-h treatments with compounds **4**, **5**, **8**, or **9**, respectively, KBM5 versus KBM5-T315I, 32D-Bcr-Abl versus 32D-T315I cells were analyzed by immunoblotting or RT-PCR. The results showed that the protein levels of Bcr-Abl were decreased by the four compounds in a dose-dependent manner (Fig. 3A). Concomitantly, the mRNA levels of Bcr-Abl were remarkably diminished (Fig. 3B). These results together indicated that derivatives of **1** inhibit Bcr-Abl at the transcriptional level leading to decreased protein levels.

Because triptolide is an inhibitor of RNA polymerase II (pol II), we examined whether these analogues possessed similar activities. As shown in Figure 3A, the phosphorylation of pol II was diminished in a dose-dependent manner in both KBM5 and KBM5-T315I cells by these analogues. Similar findings were also obtained in HeLa cells (cervical carcinoma), HCT116 (colon cancer), and Du145 (prostate carcinoma) (data not shown), indicating a general inhibitory activity of these compounds in a variety of cancer cells of different tissue origins. In aggregate, treatment with the derivatives of triptolide leads to inhibition of RNA polymerase resulting in downregulation of Bcr-Abl mRNA level and Bcr-Abl protein level regardless of mutation status the Bcr-Abl gene.

### 3.3. Compound 5 inhibited growth of the xenografted KBM5-T315I cells in nude mice

We examined the in vivo effect of compound **5** on imatinib-resistant CML cells using the nude mouse xenograft model. Four *nu/nu* BALB/c mice were injected with KBM5-T315I cells. Fourteen days after inoculation of tumor cells, when the size of tumor reached approximately 50 $mm^3$, the mice were randomized to receive treatment with normal saline (placebo) or compound **5** dissolved in normal saline, 0.5 mg/kg/d, intraperitoneally (ip), for two weeks (four animals each group). We found that this dosage was well tolerated by pilot dose-finding experiments (data not shown). The growth curves (the estimated tumor size calculated from the tumor dimension versus time) are shown in Figure 4. The data revealed that compound **5** potently inhibited the growth of KBM5-T315I tumors. The body weight of the mice remained stable, with no significant differences between treated and control mice (data not shown). Motor activity and feeding behavior of the mice were all normal. Whole blood cell counts did not reveal any significant myelosuppression in the treated mice (data not shown), nor were aspartate and alanine aminotransferase activities increased in the treatment group. No mice died. Overall, surveillance of morbidity and mortality did not reveal any significant toxicity of the compound **5** at the dosage used.

### 3.4. Molecular docking

Triptolide does not directly inhibit the activity of tyrosine kinase; rather, it inhibits the activity of RNA polymerase II (pol II).[26–28] We therefore performed the molecular docking to elucidate, at an atomic level, the potential interactions that govern the recognition and the binding of triptolide derivatives (representative compounds **4**, **5**, **8** and **9**) to pol II. To date, only the

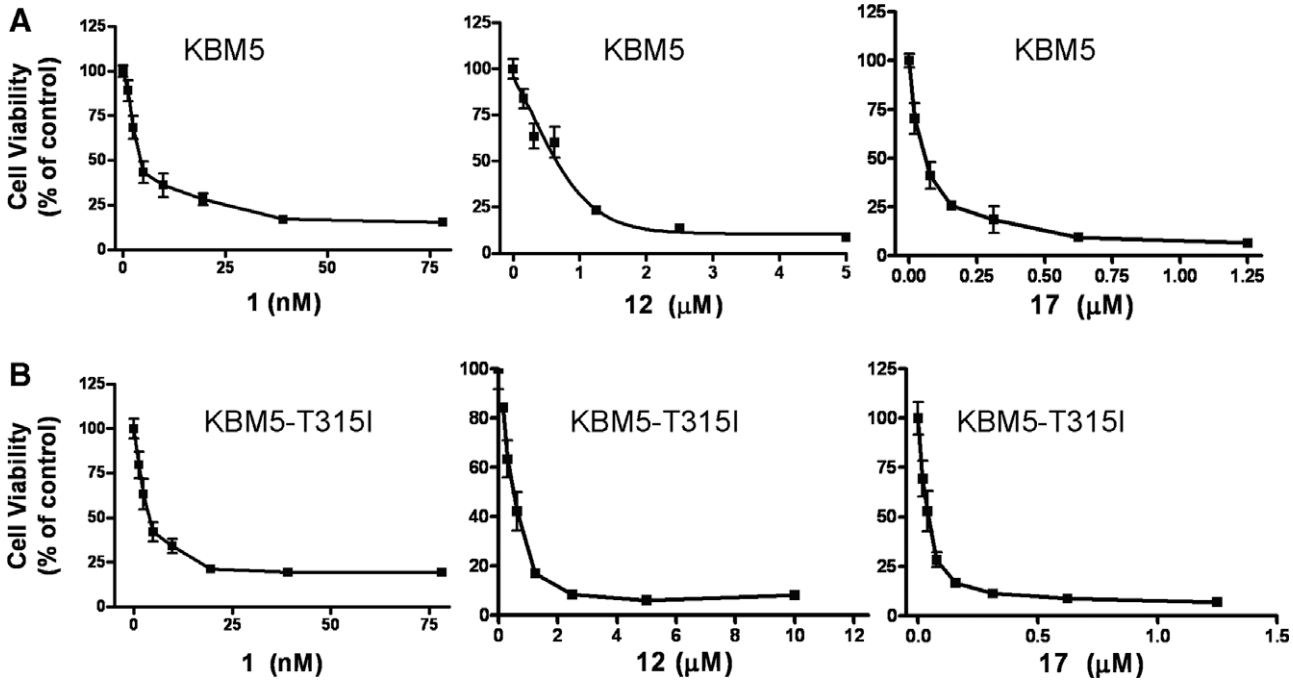


**Figure 2.** Derivatives of **1** inhibit growth of chronic myelogenous leukemia (CML) cells expressing wild-type Bcr-Abl and T315I-mutant Bcr-Abl at nanomolar concentrations. Cell viability (percent relative to control) was determined by MTS assay. Dose–response curves are shown. Error bars indicate standard errors (SE).

**Table 2**
$IC_{50}$ values of triptolide derivatives in normal cells and murine CML cells after 72-h exposure

| Compound | IC50 (nM) | | | |
|---|---|---|---|---|
| | MEF | NHFB | 32D-Bcr-Abl | 32D-T315I |
| 1 | 9200 | 8800 | 32 | 34 |
| 4 | 11,000 | 11,400 | 73 | 80 |
| 5 | 11,500 | 10,400 | 70 | 80 |
| 8 | 11,100 | 11,400 | 50 | 44 |
| 9 | 10,400 | 10,000 | 61 | 74 |

structures of subunits Rpb6, Rpb8 and the Rpb4/Rpb7 dimer have been determined by NMR and X-ray crystallography in human pol II.[37] For the fission yeast *Schizosaccharomyces pombe* showed considerable sequence homology to the subunits of the human pol II (>53%), we chose the largest subunit of *Schizosaccharomyces pombe* pol II (pdb ID: 3h0g) as the receptor to conduct the docking. The docking result showed that compound **9** had the highest score in the modeling which was in accord with the pharmacological results. The structure of the ligand (**9**)-pol II complex was shown in Figure 5.

## 4. Conclusions

The prognosis of CML resistant to imatinib is poor. Point mutations in Bcr-Abl, which prevent imatinib binding, are responsible for most of the cases of acquired clinical resistance to imatinib. In the present study, a series of novel derivatives of **1** were synthesized. We evaluated their antitumor activity with CML cells (including KBM5-T315I cells) in terms of proliferation inhibition, apoptosis, and signal transduction. Nude mouse xenograft model was also demonstrated the in vivo antitumor activity of **9**. In contrast to previous studies that aimed at improving water solubility and exploiting the structure–activity relationship of **1** via C-14 modification, we focused on increasing its effect against imatinib-resistant CML cells bearing T315I Bcr-Abl via synthesis of the series of 14-hydroxyl substituted by amine esters. Cationic amine group can facilitate the contact of bio-macromolecule with small molecules by electrostatic interaction. We synthesized a new series of C-14 triptolide derivatives with C-14-hydroxyl substituted by different amine esters (**3**–**18**).We found that the bigger the substituted group was, the weaker the antitumor effect was (compared with **7** and **16**), and that different heteroatom might give different effect (compared **4**, **5** and **6**; **10** and **14**). Taken together, the results support that the stereo-hindrance of C-14 group is important for the antitumor effect of these triptolide derivatives.

We have found a group of novel water-soluble derivatives of triptolide (**3–9**, **11–14**, **17** and **18**) with anticancer activity in vivo and in vitro.

## 5. Experimental section

### 5.1. Chemistry

Melting points (mp) were determined on X-4 micromelting point apparatus. The NMR spectra were performed on Varian Inova 300NB NMR spectrometer using TMS as an internal standard. The NMR experiments include $^{1}H$ NMR, $^{13}C$ NMR. HREIMS were measured on a Thermo MAT95XP high-resolution mass spectrometer and ABI 4800 plus MALDI-TOF/TOF. EIMS were measured on a Thermo DSQ EI-mass spectrometer. Si gel (200–300 mesh, Qingdao Haiyang Chemical Co. Ltd) was used for column chromatography (CC). Silica gel precoated aluminum cards with fluorescent indicator visualizable at 254 nm (Merck) were used for thin layer chromatography (TLC).

#### 5.1.1. 14-Chloracetyl triptolide ester (2)

Chloroacetyl chloride (0.039 mL, 0.490 mmol) was added into a mixture of triptolide (**1**) (50 mg, 0.139 mmol), 4-dimethylaminopyridine (85 mg, 0.696 mmol) in dichloromethane (1.75 mL) at 0 °C. The reaction mixture was stirred at 25 °C for 24 h and washed with HCl (5%, 10 mL × 3) and then water (10 mL × 3) successively, and then dried with anhydrous magnesium sulfate and

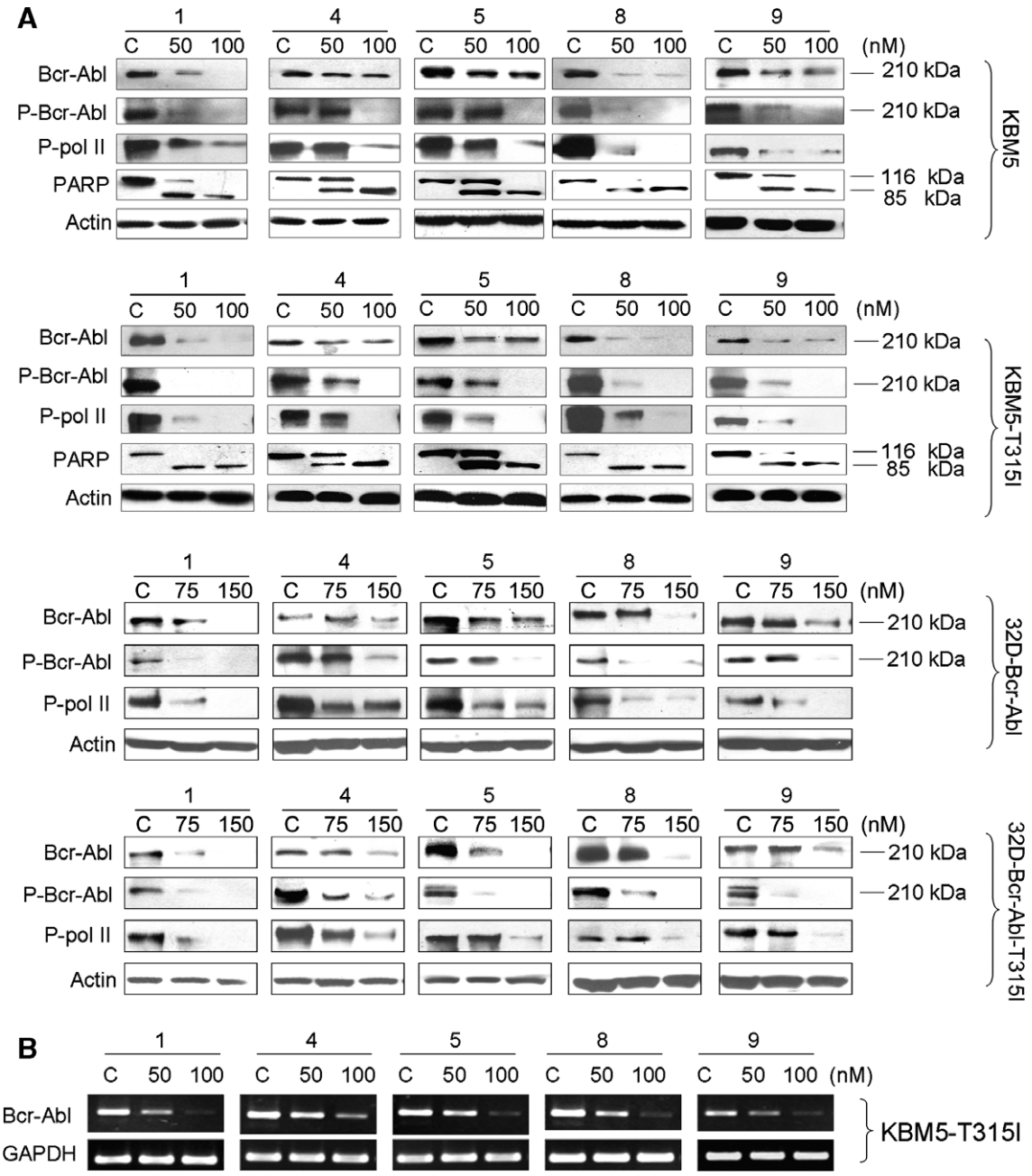


**Figure 3.** Derivatives of **1** decrease Bcr-Abl mRNA and activity of RNA polymerase II. KBM5 versus KBM5-T315I, and 32D-Bcr-Abl versus 32D-T315I cells were exposed to the derivatives of **1** at the indicated concentrations for 18 h. (A) Cell lysates were analyzed by Western blotting with the specific antibodies against the proteins as indicated, immunoblots of phospho-c-Abl, Bcr-Abl, phospho-RNA polymerase II, PARP and actin are shown. (B) Semi-quantitative analysis of RT-PCR in CML cells after 18 h of treatment with the derivatives. Ethidium bromide-stained RT-PCR products of Bcr-Abl and GAPDH mRNAs from KBM5 and KBM5-T315I cells treated with control medium or derivatives (50 nM, 100 nM) for 18 h are shown. **C** denoted control.

concentrated under reduced pressure. The resulting residue was purified by chromatography on silica gel (30 g) eluting with $CH_2Cl_2/CH_3OH$ (100:0.5), then (100:1) to give **2** (45 mg, 74.2%) as a colorless solid. Mp 122–124 °C. $^1H$ NMR ($CDCl_3$, 300 MHz) $\delta$ 5.30 (s, 1H), 5.10 (s, 1H), 4.67 (s, 2H), 4.19 (d, $J$ = 6.6 Hz, 2H), 3.84 (d, $J$ = 3 Hz, 1H), 3.56 (d, $J$ = 3 Hz, 1H), 3.49 (d, $J$ = 5.7 Hz, 1H), 2.69 (m, 1H), 2.18 (m, 2H), 1.91 (m, 2H), 1.57 (m, 1H), 1.22 (m, 1H), 1.06 (s, 3H), 0.97 (d, $J$ = 6.9 Hz, 3H), 0.86 (d, $J$ = 6.6 Hz, 3H). $^{13}C$ NMR ($CDCl_3$, 75 MHz) $\delta$ 173.0, 166.9, 159.7, 125.5, 72.89, 69.9, 63.5, 63.0, 61.4, 59.5, 55.4, 55.0, 40.9, 40.3, 35.7, 29.9, 28.1, 23.4, 17.5, 17.1, 16.7, 13.8. HREIMS $m/z$ 436.1282 (calcd for $C_{22}H_{25}O_7Cl_1$: 436.1283).

### 5.1.2. General procedure for the synthesis of compounds 3–18

Example: **triptolidyl 2-(pyrrolidin-1-yl) acetate (3).** To a solution of **14-chloracetyl triptolide ester** (**2**) (10 mg, 0.0229 mmol) in $CH_3CN$(1 mL), was added at 0 °C pyrrolidine (4.07 mg, 0.0573 mmol) in THF (0.5 mL), The reaction mixture was stirred at 25 °C for 24 h and concentrated under reduced pressure. The resulting residue was purified by chromatography on silica gel (15 g) eluting with $CH_2Cl_2$/MeOH (100:1), then (100:2) to give **3** (45 mg, 74.2%). Yield: 78% of a colorless solid. Mp 152–154 °C. $^1H$ NMR ($CDCl_3$, 300 MHz) $\delta$ 5.13 (s, 1H), 4.68 (s, 2H), 4.19 (d, $J$ = 7.2 Hz, 2H), 3.89 (d, $J$ = 3.3 Hz, 1H), 3.55 (d, $J$ = 3.3 Hz, 1H), 3.48 (d, $J$ = 5.4 Hz, 1H), 2.75 (m, 1H), 2.35 (m, 2H), 2.35 (m, 2H),

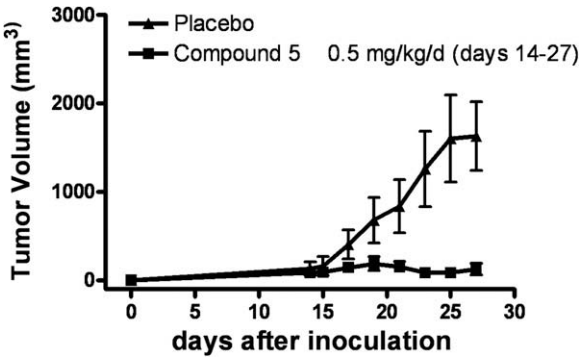


**Figure 4.** Compound **5** abrogates the growth of tumors transplanted in nude mice. The growth curves of subcutaneous xenografts of imatinib-resistant KBM5-T315I cells are shown. The estimated tumor sizes are plotted against the number of days since compound **5** treatment began (day 14 after inoculation). Placebo: normal saline. The error bars represent standard errors.

2,20 (m, 2H), 1.93 (m, 2H), 1.90 (m, 2H), 1.90 (m, 2H),1.85 (m, 1H), 1.58 (m, 1H), 1.26 (s, 1H), 1.06 (s, 3H), 0.97 (d, $J$ = 6.9 Hz, 3H), 0.86 (d, $J$ = 6.9 Hz, 3H). $^{13}$C NMR ($CDCl_3$, 75 MHz) $\delta$ 173.0, 162.2, 159.9, 125.4, 71.0, 70.0, 63.5, 63.3, 61.2, 59.6, 55.4, 55.0, 53.6, 53.6, 40.4, 40.3, 35.7, 29.9, 28.0, 23.5, 23.5, 23.4, 17.6, 17.1, 16.7, 13.8. HREIMS $m/z$ 471.2253 (calcd for $C_{26}H_{33}O_7N_1$: 471.2252).

### 5.1.3. Triptolidyl 2-(1-methylpiperidine-1-yl) acetate (4)

Yield: 83% of a colorless solid. Mp 122–124 °C. $^1$H NMR ($CDCl_3$, 300 MHz) $\delta$ 5.12 (s, 1H), 4.67 (s, 2H), 3.83 (d, $J$ = 3.0 Hz, 1H), 3.53 (d, $J$ = 2.7 Hz, 1H), 3.47 (d, $J$ = 5.7 Hz, 1H), 3.33 (d, $J$ = 6.3 Hz, 2H), 2.65 (m, 1H), 2.57 (m, 2H), 2.57 (m, 2H), 2.17 (m, 2H), 1.95 (s, 1H), 1.90 (m, 2H), 1.85 (s, 1H), 1.64 (m, 2H), 1.64 (m, 2H), 1.45 (m, 2H), 1.26 (s, 1H), 1.00 (s, 3H), 1.06 (s, 3H), 0.97 (d, $J$ = 6.9 Hz, 3H), 0.85 (d, $J$ = 6.9 Hz, 3H). $^{13}$C NMR ($CDCl_3$, 75 MHz) $\delta$ 172.9, 162.6, 159.8, 125.5, 70.9, 69.9, 63.6, 63.3, 61.2, 59.6, 55.4, 55.1, 53.9, 53.9, 40.4, 40.3, 35.7, 29.9, 28.2, 25.9, 25.9, 23.9, 23.4, 17.6, 17.1, 16.7, 13.8. HREIMS $m/z$ 485.2409 (calcd for $C_{27}H_{35}O_7N_1$: 485.2408).

### 5.1.4. Triptolidyl 2-(morpholine-1-yl) acetate (5)

Yield: 75% of a colorless solid. Mp 98–99 °C. $^1$H NMR ($CDCl_3$, 300 MHz) $\delta$ 5.13 (s, 1H), 4.67 (s, 2H), 3.83 (d, $J$ = 3.0 Hz, 1H), 3.76 (t, $J$ = 4.5 Hz, 2H), 3.76 (t, $J$ = 4.5 Hz, 2H), 3.54 (d, $J$ = 3.0 Hz, 1H), 3.48 (dd, $J$ = 5.7 Hz, 1H), 3.35 (q, $J$ = 16.5 Hz, 28.2 Hz, 2H), 2.68 (m, 1H), 2.64 (m, 2H), 2.64 (m, 2H), 2.17 (m, 2H), 1.90 (m, 2H), 1.56 (m, 1H), 1.45 (m, 2H), 1.26 (s, 1H), 1.21 (m, 1H), 1.01 (s, 3H), 0.98 (d, $J$ = 6.9 Hz, 3H), 0.86 (d, $J$ = 6.9 Hz, 3H). $^{13}$C NMR ($CDCl_3$, 75 MHz) $\delta$ 173.0, 169.5, 159.7, 125.5, 71.2, 69.9, 66.9, 66.9, 63.6, 63.2, 61.3 , 59.7, 59.6, 55.5, 55.1, 53.1, 53.1, 40.4, 35.8, 29.9, 28.3, 23.6, 17.6, 17.2, 16.8, 13.8. HREIMS $m/z$ 487.2200 (calcd for $C_{26}H_{33}O_8N_1$: 487.2201).

### 5.1.5. Triptolidyl 2-(1-methylpiperazine-1-yl) acetate (6)

Yield: 75% of a colorless oil; $^1$H NMR ($CDCl_3$, 300 MHz) $\delta$ 5.11 (s, 1H), 4.67 (s, 2H), 4.21 (m, 1H), 3.83 (d, $J$ = 3.3 Hz, 1H), 3.54 (d, $J$ = 3.0 Hz, 1H), 3.47 (d, $J$ = 5.4 Hz, 1H), 3.35 (d, $J$ = 16.8 Hz, 29.4 Hz, 2H),2.70 (m, 2H), 2.37 (s, 1H), 2.37 (m, 2H), 2.17 (m, 2H) , 2.15 (m, 2H), 1.90 (m, 2H), 1.56 (m, 1H), 1.45 (m, 2H), 1.27 (m, 1H), 1.26 (s, 3H), 1.05 (s, 3H), 0.96 (d, $J$ = 6.9 Hz, 3H), 0.84 (d, $J$ = 6.9 Hz, 3H). $^{13}$C NMR ($CDCl_3$, 75 MHz) $\delta$ 173.2, 168.9, 159.7, 125.5 , 71.2, 69.9, 63.5, 63.2, 61.3, 59.6, 55.4, 55.0, 54.6, 54.6, 52.3, 52.3, 45.6, 40.4, 40.3, 35.7, 29.9, 29.7, 23.5, 17.3, 17.1, 16.8, 13.8. HREIMS $m/z$ 500.2515 (calcd for $C_{27}H_{36}O_7N_2$: 500.2517).

### 5.1.6. Triptolidyl 2-(butan-1-amine-1-yl) acetate (7)

Yield: 95% of a colorless solid. Mp 114–116 °C.$^1$H NMR ($CDCl_3$, 300 MHz) $\delta$ 5.30 (s, 1H), 5.10 (s, 1H), 4.67 (s, 2H), 4.25 (q, $J$ = 15 Hz, 22.2 Hz, 2H), 3.84 (d, $J$ = 3.3 Hz, 1H), 3.72 (d, $J$ = 3.3 Hz, 1H), 3.56 (d, $J$ = 3 Hz, 1H), 3.49 (q, $J$ = 6.0 Hz, 12.0 Hz, 1H), 2.87 (m, 2H), 2.69 (m, 1H), 2.35 (m, 1H), 2.30 (m, 1H), 2.17 (m, 2H), 1.91 (m, 2H), 1.59 (d, $J$ = 4.8 Hz, 1H), 1.59 (d, $J$ = 4.5 Hz, 1H), 1.57 (m, 1H), 1.26 (m, 2H), 1.26 (s, 2H), 1.06 (s, 3H), 0.97 (d, $J$ = 6.9 Hz, 3H), 0.86 (d, $J$ = 6.6 Hz, 3H). $^{13}$C NMR ($CDCl_3$, 75 MHz) $\delta$ 173.1, 166.9, 159.7, 125.5, 72.87, 69.9, 63.5, 63.2, 63.2, 61.4, 61.2, 59.6, 59.5, 55.4, 55.0, 40.9, 40.3, 35.7, 29.9, 29.7, 28.0, 23.4, 17.5, 17.1, 16.7, 13.8. HREIMS $m/z$ 473.2399 (calcd for $C_{26}H_{35}O_7N_1$, 473.2408).

### 5.1.7. Triptolidyl 2-(amine-1-yl) acetate (8)

Yield: 90% of a colorless solid. Mp 223–225 °C .$^1$H NMR ($CDCl_3$, 300 MHz) $\delta$ 4.68 (s, 2H), 3.91 (d, $J$ = 3.3 Hz, 2H), 3.52 (d, $J$ = 2.4 Hz, 1H), 3.42 (d, $J$ = 10.5 Hz, 1H), 3.38 (d, $J$ = 5.4 Hz, 1H), 2.74 (d, $J$ = 10.8 Hz, 1H), 2.32 (m, 1H), 2.23 (m, 1H), 2.16 (t, $J$ = 5.7 Hz, 1H), 1.99 (d, $J$ = 13.2 Hz, 1H), 1.61 (s, 2H), 1.56 (m, 2H), 1.23 (m, 2H), 1.13 (s, 3H), 1.02 (d, $J$ = 6.9 Hz, 3H), 0.90 (d, $J$ = 6.9 Hz, 3H). $^{13}$C NMR ($CDCl_3$) $\delta$ 173.0, 173.0, 160.0, 125.4, 73.4, 69.9, 66.2, 65.7, 60.8, 60.1, 56.8, 54.6, 40.5, 40.5, 35.8, 29.9, 28.3, 23.8, 17.8, 17.2, 16.9, 13.8, HREIMS $m/z$ 417.1809 (calcd for $C_{22}H_{27}O_7N_1$: 417.1782).

### 5.1.8. Triptolidyl 2-(aminomethanol-1-yl) acetate (9)

Yield: 85% of a colorless solid. Mp 131–133 °C. $^1$H NMR ($CDCl_3$, 300 MHz) $\delta$ 4.68 (s, 2H), 3.90 (s, 1H), 3.86 (m, 2H), 3.52 (m, 2H), 3.56 (d, $J$ = 3 Hz, 1H), 3.42 (m, 1H), 3.38 (d, J = 5.4 Hz, 1H), 2.70

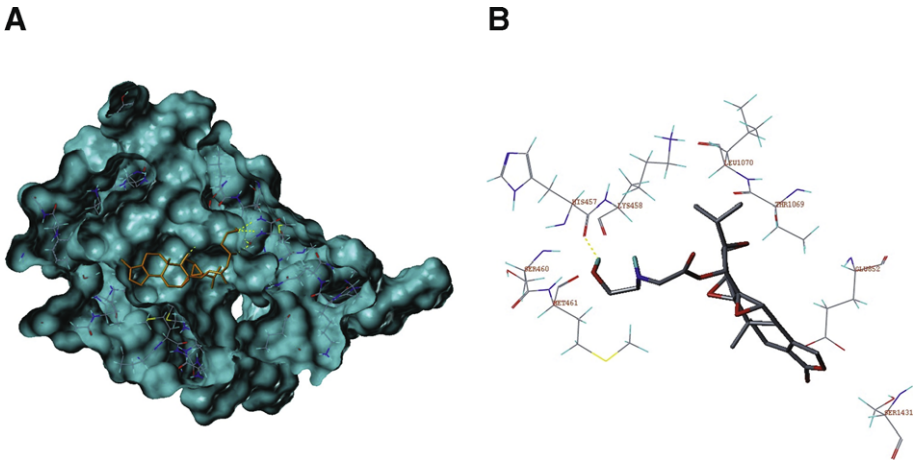


**Figure 5.** Molecular docking analysis of RNA polymerase II to derivative **9**. (A) Docking pocket of protein with compound **9** (orange color). Opaque type surface was created of the active site. (B) Details interaction between compound **9** to protein with some residues labeled.

(m, 2H), 2.36 (m, 1H), 2.30 (m, 1H), 2.23 (m, 1H), 2.16 (m, 2H), 1.97 (s, 1H), 1.90 (m, 1H), 1.57 (dd, $J$ = 5.1, 12.3 Hz, 1H), 1.26 (s, 1H), 1.20 (m, 1H), 1.13 (s, 3H), 1.02 (d, $J$ = 6.9 Hz, 3H), 0.89 (d, $J$ = 6.9 Hz, 3H). $^{13}$C NMR ($CDCl_3$, 75 MHz) $\delta$ 173.7, 170.2, 159.7, 125.5, 73.5, 69.9, 66.2, 65.7, 60.7, 60.1, 59.7, 56.7, 55.6, 54.5, 40.5, 40.2, 35.8, 29.9, 28.3, 23.7, 17.8, 17.1, 16.9, 13.7. MS: 462.1913 (calcd for $C_{24}H_{31}O_8N_1$)

### 5.1.9. Triptolidyl 2-(4-chloroaniline-1-yl) acetate (10)

Yield: 55% of a yellow solid. Mp 95–97 °C. $^1$H NMR ($CDCl_3$, 300 MHz) $\delta$ 7.13 (d, $J$ = 9 Hz, 1H), 7.13 (d, $J$ = 9 Hz, 1H), 6.56 (d, $J$ = 9 Hz, 1H), 6.56 (d, $J$ = 9 Hz, 1H), 5.11 (s, 1H), 4.70 (s, 2H), 4.19 (q, $J$ = 15.0, 21.6 Hz, 2H), 3.84 (d, $J$ = 3 Hz, 1H), 3.56 (d, $J$ = 3 Hz, 1H), 3.49 (d, $J$ = 5.7 Hz, 1H), 2.69 (m, 1H), 2.35 (m, 1H), 2.16 (m, 2H), 1.92 (m, 2H), 1.57 (m, 1H), 1.26 (m, 2H), 1.07 (s, 3H), 0.98 (d, $J$ = 6.9 Hz, 3H), 0.86 (d, $J$ = 6.9 Hz, 3H). $^{13}$C NMR ($CDCl_3$, 75 MHz) $\delta$ 172.9, 166.9, 159.6, 145.4, 129.0, 129.0, 125.6, 114.2, 109.7, 109.7, 73.0, 69.9, 63.5, 63.1, 61.4, 59.5, 55.4, 55.3, 40.8, 40.4, 35.7, 29.9, 28.1, 23.5, 17.5, 17.2, 16.8, 13.9. HREIMS $m/z$ 527.1716 (calcd for $C_{28}H_{30}O_7N_1Cl_1$: 527.1705).

### 5.1.10. Triptolidyl 2-(methyl 2-aminopropanoate-1-yl) acetate (11)

Yield: 75% of a colorless solid. Mp 110–112 °C. $^1$H NMR ($CDCl_3$, 300 MHz) $\delta$ 5.30 (s, 1H), 5.11 (s, 1H), 4.68 (s, 2H), 4.19 (q, $J$ = 15.0, 21.9 Hz, 2H), 3.85 (d, $J$ = 3 Hz, 1H),3.74 (s, 1H), 3.57 (d, $J$ = 3 Hz, 1H), 3.50 (d, $J$ = 5.7 Hz, 1H), 3.47 (s, 3H), 2.69 (m, 1H), 2.17 (m, 2H), 1.92 (m, 2H), 1.92 (s, 1H), 1.8 (s, 1H),1.57 (dd, $J$ = 4.2, 13.2 Hz, 1H), 1.26 (s, 3H), 1.06 (s, 3H), 0.98 (d, $J$ = 6.9 Hz, 3H), 0.86 (d, $J$ = 6.6 Hz, 3H). $^{13}$C NMR ($CDCl_3$, 75 MHz) $\delta$ 175.4, 173.9, 169.7, 157.5, 125.6, 72.9, 69.9, 63.5, 63.0, 61.4, 60.0, 59.5, 55.4, 55.0, 40.9, 40.3, 38.8, 35.7, 29.9, 29.6, 28.1, 23.4, 17.5, 17.1, 16.7, 13.8. HREIMS $m/z$ 503.2151 (calcd for $C_{26}H_{33}O_9N_1$, 503.2150).

### 5.1.11. Triptolidyl 2-(ethane-1,2-diamine-1-yl) acetate (12)

Yield: 80% of a colorless solid. Mp 130–132 °C. $^1$H NMR ($CDCl_3$, 300 MHz) $\delta$ 5.13 (s, 2H), 4.68 (s, 2H), 3.84 (d, $J$ = 3.3 Hz, 1H), 3.75 (s, 1H), 3.55 (d, $J$ = 3.0 Hz, 1H), 3.50 (s, 1H), 3.49 (s, 1H), 3.46 (d, $J$ = 7.2 Hz, 2H), 3.41 (d, $J$ = 5.4 Hz, 2H), 2.93 (m, 1H), 2.93 (m, 1H), 2.70 (m, 2H), 2.16 (m, 2H), 1.91 (m, 2H), 1.61 (s, 1H), 1.27 (m, 1H), 1.05 (s, 3H), 0.99 (d, $J$ = 6.9 Hz, 3H), 0.86 (d, $J$ = 6.9 Hz, 3H). $^{13}$C NMR ($CDCl_3$, 75 MHz) $\delta$ 173.3, 169.4, 159.7, 125.9, 71.6, 69.9, 63.6, 63.1, 61.5, 59.7, 55.6, 55.0, 48.3, 41.6, 40.3, 37.2, 35.7, 29.9, 28.3, 23.5, 17.6, 17.2, 16.8, 13.8. HREIMS $m/z$ 460.2217 (calcd for $C_{24}H_{32}O_7N_2$, 460.2204).

### 5.1.12. Triptolidyl 2-(piperazine-1-yl) acetate (13)

Yield: 75% of a colorless solid. Mp 230–232 °C. $^1$H NMR ($CDCl_3$, 300 MHz) $\delta$ 5.10 (s, 1H), 4.67 (s, 2H), 3.84 (d, $J$ = 3.3 Hz, 1H), 3.55 (d, $J$ = 2.7 Hz, 1H), 3.50 (d, $J$ = 4.8 Hz, 2H), 3.43 (s, 1H), 3.38 (s, 1H), 3.29 (m, 2H), 3.29 (m, 2H), 2.96 (m, 2H), 2.96 (m, 2H), 2.70 (m, 1H), 2.15 (m, 2H), 1.91 (m, 2H), 1.58 (dd, $J$ = 4.8, 12.6 Hz, 1H), 1.27 (s, 1H), 1.22 (m, 1H), 1.03 (s, 3H), 0.97 (d, $J$ = 6.9 Hz, 3H), 0.86 (d, $J$ = 6.9 Hz, 3H). $^{13}$C NMR ($CDCl_3$, 75 MHz) $\delta$ 172.9, 168.9, 159.6, 125.6, 71.7, 69.9, 63.5, 63.1, 61.5, 59.8, 58.7, 55.6, 55.1, 49.4, 49.4, 43.6, 43.6, 40.4, 35.7, 30.0, 28.4, 23.5, 17.6, 17.2, 16.8, 13.9. HREIMS $m/z$ 486.2364 (calcd for $C_{26}H_{34}O_7N_2$: 486.2361).

### 5.1.13. 4-(Pyridin-3-yl)pyrimidin-2-amine

4-(Pyridin-3-yl)pyrimidin-2-amine was synthesized follow the literature. Yield 90% of three steps of a pale yellow slice. Mp 172 °C (sublimation), $^1$H NMR (MeOD, 300 MHz) $\delta$ 9.20 (s, 1H), 8.62 (s, 1H), 8.49 (s, 1H), 8.32 (s, 1H), 7.55 (s, 1H), 7.17 (s, 1H). $^{13}$C NMR (MeOD, 75 MHz) $\delta$ 163.9, 160.0, 151.6, 149.2, 148.8, 136.5, 134.6, 125.2, 107.6. HREIMS $m/z$ 172.0740 (calcd for $C_9H_8N_4$, 172.0743).

### 5.1.14. Triptolidyl 2-(4-(pyridin-3-yl)pyrimidin-2-amine-1-yl) acetate (14)

Yield: 70% of a colorless solid. Mp 167–169 °C. $^1$H NMR ($CDCl_3$, 300 MHz) $\delta$ 9.23 (s, 1H), 8.73 (d, $J$ = 3.3 Hz, 1H), 8.43 (d, $J$ = 5.1 Hz, 1H), 8.30 (d, $J$ = 7.8 Hz, 1H), 7.40 (m, 1H), 7.06 (d, $J$ = 4.2 Hz, 1H), 5.18 (s, 1H), 4.68 (s, 2H), 3.90 (d, $J$ = 3 Hz, 1H), 3.52 (d, $J$ = 2.1 Hz, 1H), 3.42 (m, 2H), 3.38 (d, $J$ = 5.1 Hz, 1H), 2.69 (m, 1H), 2.28 (m, 1H), 2.18 (m, 2H), 1.91 (m, 2H), 1.70 (s, 1H), 1.57 (m, 1H), 1.22 (m, 1H), 1.13 (s, 3H), 1.02 (d, $J$ = 6.9 Hz, 3H), 0.90 (d, $J$ = 6.6 Hz, 3H). $^{13}$C NMR ($CDCl_3$, 75 MHz) $\delta$ 173.0, 166.7, 163.2, 162.8, 159.1, 151.2, 149.4, 148.2 134.3, 132.7, 125.5, 123.5, 107.6, 73.5, 69.9, 66.2, 60.8, 60.1, 56.8, 54.6, 55.0, 40.5, 40.1, 35.8, 29.9 , 28.3, 23.8, 17.8, 17.2, 17.0, 13.7. MS $m/z$ 573.2217 (calcd for $C_{31}H_{32}O_7N_4$).

### 5.1.15. Triptolidyl 2-(2,2′-azanediyldiethanol-1-yl) acetate (15)

Yield: 70% of a colorless oil. $^1$H NMR ($CDCl_3$, 300 MHz) $\delta$ 4.69 (s, 2H), 4.55 (s, 1H), 4.19 (d, $J$ = 3.9 Hz, 2H), 3.90 (s, 1H), 3.90 (s, 1H), 3.83 (m, 2H), 3.83 (m, 2H), 3.56 (m, 1H), 3.50 (s, 2H), 3.49 (m, 1H), 2.27 (m, 2H), 2.27 (m, 2H), 2.69 (m, 1H), 2.18 (m, 2H), 1.91 (m, 2H), 1.57 (m, 1H), 1.22 (m, 1H), 1.06 (s, 3H), 0.88 (d, $J$ = 6.9 Hz, 3H), 0.81 (d, $J$ = 6.6 Hz, 3H). $^{13}$C NMR ($CDCl_3$, 75 MHz) $\delta$ 173.3, 166.7, 160.2, 125.5, 73.44, 68.0, 63.8, 63.0, 62.2, 62.2, 61.1, 60.6, 60.6, 59.2, 55.7, 55.6, 47.8, 40.3, 35.3, 29.9, 28.1, 23.7, 17.7, 17.1, 16.5, 13.7. MS $m/z$ 506.1972 (calcd for $C_{26}H_{35}O_9N_1$).

### 5.1.16. Triptolidyl 2-(dodecan-1-amine-1-yl) acetate (16)

Yield: 80% of a colorless oil. $^1$H NMR ($CDCl_3$, 300 MHz) $\delta$ 5.12 (s, 1H), 4.67 (s, 2H), 4.31 (t, $J$ = 6.6 Hz, 1H), 4.09 (d, $J$ = 6.6 Hz, 1H), 3.83 (d, $J$ = 3 Hz, 1H), 3.57 (s, 1H), 3.54 (d, $J$ = 3 Hz, 1H), 3.49 (d, $J$ = 6.0 Hz, 1H), 2.66 (m, 1H), 2.64 (m, 1H) 2.16 (m, 2H), 1.91 (m, 2H), 1.77 (m, 2H),1.57 (m, 1H), 1.52 (m, 2H), 1.26 (s, 2H), 1.26 (s, 2H), 1.26 (s, 2H), 1.26 (s, 2H), 1.26 (s, 2H), 1.26 (s, 2H), 1.26 (s, 2H), 1.26 (s, 2H), 1.22 (m, 1H), 1.06 (s, 3H), 1.01 (s, 3H), 0.97 (d, $J$ = 6.9 Hz, 3H), 0.86 (d, $J$ = 6.6 Hz, 3H). $^{13}$C NMR ($CDCl_3$, 75 MHz) $\delta$ 173.5, 166.1, 160.0, 125.8, 72.9, 71.9, 66.2, 61.8, 61.7, 58.6, 56.2, 53.2, 48.1 , 40.6, 40.2, 35.9, 30.2, 30.0, 30.0, 30.0, 30.0, 30.0, 30.0, 30.0, 30.0, 29.4, 28.8, 23.8, 23.0, 17.5, 15.9, 15.5, 14.5, 14.4. HREIMS $m/z$ 585.3660 (calcd for $C_{34}H_{51}O_7N_1$, 585.3660).

### 5.1.17. Triptolidyl 2-(diethylamine-1-yl) acetate (17)

Yield: 70% of a colorless solid. Mp 50–52 °C. $^1$H NMR ($CDCl_3$, 300 MHz) $\delta$ 5.11 (s, 1H), 4.67 (s, 2H), 3.83 (d, $J$ = 3 Hz, 1H), 3.54 (d, $J$ = 3 Hz, 1H), 3.49 (t, $J$ = 5.7 Hz, 2H), 2.75 (m, 2H), 2.75 (m, 2H), 2.69 (m, 1H), 2.32 (m, 2H), 2.18 (m, 2H), 1.91 (m, 2H), 1.57 (m, 1H), 1.22 (m, 1H), 1.12 (t, $J$ = 7.2 Hz, 3H), 1.12 (t, $J$ = 7.2 Hz, 3H), 1.07 (s, 3H), 0.98 (d, $J$ = 6.9 Hz, 3H), 0.86 (d, $J$ = 6.9 Hz, 3H). $^{13}$C NMR ($CDCl_3$, 75 MHz) $\delta$ 173.0, 170.5, 159.8, 125.6, 73.4, 69.9, 63.6, 63.3, 61.2, 59.7, 55.4, 55.1, 53.7, 53.7, 47.6, 40.5, 35.8, 29.9, 28. 2, 23.6 17.6, 17.2, 16.8, 13.8, 12.5, 12.5. HREIMS $m/z$ 473.2407 (calcd for $C_{26}H_{35}O_7N_1$: 473.2408).

### 5.1.18. Triptolidyl 2-(methanamine-1-yl) acetate (18)

Yield: 85% of a colorless solid. Mp 109–111 °C. $^1$H NMR ($CDCl_3$, 300 MHz) $\delta$ 5.13 (s, 1H), 4.68 (s, 2H), 4.31 (t, $J$ = 6.6 Hz, 2H), 3.90 (s, 1H), 3.84 (d, $J$ = 3.0 Hz, 1H), 3.76 (m, 3H), 3.56 (d, $J$ = 3 Hz, 1H), 3.37 (d, $J$ = 5.7 Hz, 1H), 2.77 (m, 1H), 2.69 (s, 1H), 2.16 (m, 2H), 1.94 (m, 2H), 1.60 (m, 1H), 1.27 (m, 1H), 1.06 (s, 3H), 0.97 (d, $J$ = 6.9 Hz, 3H), 0.86 (d, $J$ = 6.9 Hz, 3H). $^{13}$C NMR ($CDCl_3$, 75 MHz) $\delta$ 173.8, 167.7, 158.0, 125.6, 84.1, 71.8, 69.9, 64.3, 63.9, 61.4, 59.6, 57.6, 55.4, 47.6, 39.9, 35.7, 29.8, 27.7, 23.4, 17.2, 17.2, 15.3, 14.2, HREIMS $m/z$ 431.1939 (calcd for $C_{23}H_{29}O_7N_1$: 431.1939).

### 5.2. Molecular modeling

All molecular studies were performed on a HP xw6600 workstation with Intel Xeon E5430 2.66 GHz processor running Red Hat LINUX enterprise 5 and SYBYL8.1. The crystal structure was downloaded from the PDB (http://www.rcsb.org) (PDB ID code: 3H0G). Firstly, we deleted all chains except chain A of the protein and chain A was used in the study. Secondly, hydrogen atoms were added to the protein. Ligand structures were built with SYBYL8.1 [SYBYL8.1 (Tripos, Inc., St. Louis, MO)] and minimized with the Powell method and MMFF94 force field until a rmsd gradient of 0.005 kcal/(mol Å) was reached. Docking calculations were performed using surflex-dock of SYBYL8.1 and the sfxc mode was chosen with default values. The protocol was produced based on the automatic mode and C-score calculations were performed.

### 5.3. Bioactivity assay

#### 5.3.1. Cell lines

KBM5 and KBM5-T315I cells were cultured as described previously.[30,36] In brief, KBM5 cells expressing 210 kDa wild-type Bcr-Abl were cultured in Iscove's modified Dulbecco's medium (Invitrogen, Guangzhou, China) supplemented with 10% heat-inactivated fetal calf serum (FCS). KBM5-T315I cells were routinely maintained in the same medium but with 1 μM imatinib, which was removed before experiments with a wash-out period of 2–3 days. KBM5 cells expressing the 210 kDa wild-type Bcr-Abl was derived from a female CML patient. The KBM5-T315I subline was originally established by exposure to increasing concentrations of imatinib. KBM5-T315I cells, harboring a threonine-to-isoleucine substitution at position 315 of Abl, are resistant to imatinib, and they only have a marginal increase Bcr-Abl gene copies and expression.[38–40] The 32D myeloid cells stably expressing either 210 kDa wild-type Bcr-Abl (32D-Bcr-Abl) or T315I Bcr-Abl (32D-T315I) were established and maintained in RPMI 1640 with 10% fetal bovine serum as described previously.[41] MEF (normal murine embryonic fibroblast) and NHFB (normal human fibroblast) cells were cultured in DMEM supplemented with 10% fetal calf serum.[41]

#### 5.3.2. Cell viability assay

Cell viability was evaluated by 3-(4,5-dimethyl-2-yl)-5-(3-carboxymethoxyphenyl)-2-(4-sulfophenyl)-2*H*-tetrazolium (MTS) assay (CellTiter 96 Aqueous One Solution reagent, Promega, Shanghai, China) as described previously.[42] The optical density was read on a 96 well plate reader at a single wavelength of 490 nm. The drug concentration resulting in a 50% inhibition of cell proliferation ($IC_{50}$) was determined.

#### 5.3.3. Western blot analysis

Western blot analysiswas performed using whole cell lysates prepared in RIPA buffer (1 × PBS, 1% NP-40, 0.5% sodium deoxycholate, 0.1% SDS) supplemented with freshly added 10 mM β-glycerophosphate, 1 mM sodium orthovanadate, 10 mM NaF, 1 mM phenylmethylsulfonyl fluoride, and 1 × Roche Complete Mini Protease Inhibitor Cocktail (Roche, Indianapolis, IN).[43] Antibodies against c-Abl (C-19) were from Santa Cruz Biotechnology (Santa Cruz, CA). Antibody against poly(adenosine diphosphate [ADP]-ribose) polymerase (PARP, clone 4C10-5) was from BD Biosciences (San Jose, CA). Antibodies against phospho-c-Abl at Y245 were from Cell Signaling Technology (Beverly, MA). Mouse monoclonal antibody against actin was from Sigma-Aldrich (St. Louis, MO). Anti-mouse immunoglobulin G and anti-rabbit immunoglobulin G horseradish peroxidase-conjugated antibodies were from Pierce Biotechnology (Rockford, IL).

#### 5.3.4. Semi-quantitative RT-PCR

Total RNA was extracted from KBM5 and KBM5-T315I cells treated with or without triptolide using Trizol reagent (Invitrogen). After quantification by spectrophotometry, the first-strand cDNA was synthesized from 1 μL of total RNA with the use of the RNA PCR Kit (AMV) Ver.3.0 (TaKaRa, Dalian, China) and random primers. Bcr-Abl gene amplification involved the following primers[38]: forward 5′-TTCAGAAGCTTCTCCCTGACAT-3′ (exon 13 of Bcr gene), reverse 5′-CTTCGTCTGAGATACTGGATTCCT-3′ (exon 9 of Abl gene), with an expected PCR product of 1614 bp. The PCR products were electrophoresed on 1% agarose gel.

#### 5.3.5. Nude mouse xenograft model

*nu/nu* BALB/c mice were bred at the animal facility of Sun Yat-sen University. The mice were housed in barrier facilities with a 12-h light dark cycle, with food and water available ad libitum. $3 \times 10^7$ of KBM5-T315I cells were inoculated subcutaneously on the flanks of 6–8-week-old male nude mice. Tumors were measured every other day with use of calipers. Tumor volumes were calculated by the following formula: $a^2 \times b \times 0.4$, where $a$ is the smallest diameter and $b$ is the diameter perpendicular to $a$. Compound **5** was dissolved in normal saline. Mice in the control group received the same volume of normal saline. The body weight, feeding behavior and motor activity of each animal were monitored as indicators of general health. At the end of the experiments, blood samples were collected for assay of lactate dehydrogenase, and aspartate and alanine aminotransferase activity, and complete blood count. The animals were then euthanized, and tumor xenografts were immediately removed, weighed, stored and fixed. All animal studies were conducted with the approval of the Sun Yat-sen University Institutional Animal Care and Use Committee.

### Acknowledgements

This study was supported by grants from the Major Research Plan of the National Natural Science Fund of China (Grant 90713036 to J. Pan), the National High Technology Research and Development Program of China (863 Program Grant 2008AA02Z420 to J. Pan), the National Basic Research Program of China (973 Program Grant 2009CB825506 to J. Pan), and China Postdoctoral Science Foundation (Grant 20080440794 to F.X.).

### References and notes

1. Faderl, S.; Talpaz, M.; Estrov, Z.; O'Brien, S.; Kurzrock, R.; Kantarjian, H. M. *N. Engl. J. Med.* **1999**, *341*, 164.
2. Ren, R. *Nat. Rev. Cancer* **2005**, *5*, 172.
3. Melo, J. V.; Barnes, D. J. *Nat. Rev. Cancer* **2007**, *7*, 441.
4. Quintas-Cardama, A.; Kantarjian, H.; Cortes, J. *Nat. Rev. Drug Disc.* **2007**, *6*, 834.
5. Baselga, J.; Arribas, J. *Nat. Med.* **2004**, *10*, 786.
6. Druker, B. J. *N. Engl. J. Med.* **2006**, *354*, 2594.
7. Druker, B. G. F.; O'Brien, S.; Larson, R. *J. Clin. Oncol.* **2006**, *24*, 18S.
8. Donato, N. J.; Wu, J. Y.; Stapley, J.; Gallick, G.; Lin, H.; Arlinghaus, R.; Talpaz, M. *Blood* **2003**, *101*, 690.
9. Gambacorti-Passerini, C.; le Coutre, P.; Zucchetti, M.; D'Incalci, M. *Blood* **2002**, *100*, 367.
10. Thomas, J.; Wang, L.; Clark, R. E.; Pirmohamed, M. *Blood* **2004**, *104*, 3739.
11. Gorre, M. E.; Mohammed, M.; Ellwood, K.; Hsu, N.; Paquette, R.; Rao, P. N.; Sawyers, C. L. *Science* **2001**, *293*, 876.
12. Cortes, J.; Kantarjian, H. *J. Clin. Oncol.* **2005**, *23*, 6316.
13. Azam, M.; Latek, R. R.; Daley, G. Q. *Cell* **2003**, *112*, 831.
14. Kantarjian, H. M.; Talpaz, M.; Giles, F.; O'Brien, S.; Cortes, J. *Ann. Int. Med.* **2006**, *145*, 913.
15. Morinaga, K.; Yamauchi, T.; Kimura, S.; Maekawa, T.; Ueda, T. *Int. J. Cancer* **2008**, *122*, 2621.
16. Talpaz, M.; Shah, N. P.; Kantarjian, H.; Donato, N.; Nicoll, J.; Paquette, R.; Cortes, J.; O'Brien, S.; Nicaise, C.; Bleickardt, E.; Blackwood-Chirchir, M. A.; Iyer, V.; Chen, T. T.; Huang, F.; Decillis, A. P.; Sawyers, C. L. *N. Engl. J. Med.* **2006**, *354*, 2531.
17. Chen, R.; Gandhi, V.; Plunkett, W. *Cancer Res.* **2006**, *66*, 10959.
18. Nimmanapalli, R.; Fuino, L.; Bali, P.; Gasparetto, M.; Glozak, M.; Tao, J.; Moscinski, L.; Smith, C.; Wu, J.; Jove, R.; Atadja, P.; Bhalla, K. *Cancer Res.* **2003**, *63*, 5126.

19. Corson, T. W.; Crews, C. M. *Cell* **2007**, *130*, 769.
20. Efferth, T.; Li, P. C.; Konkimalla, V. S.; Kaina, B. *Trends Mol. Med.* **2007**, *13*, 353.
21. Tao, X.; Schulze-Koops, H.; Ma, L.; Cai, J.; Mao, Y.; Lipsky, P. E. *Arthritis Rheum.* **1998**, *41*, 130.
22. Jiang, X. *Pediatr. Nephrol.* **1994**, *8*, 343.
23. Kupchan, S. M.; Court, W. A.; Dailey, R. G., Jr.; Gilmore, C. J.; Bryan, R. F. *J. Am. Chem. Soc.* **1972**, *94*, 7194.
24. Carter, B. Z.; Mak, D. H.; Schober, W. D.; McQueen, T.; Harris, D.; Estrov, Z.; Evans, R. L.; Andreeff, M. *Blood* **2006**, *108*, 630.
25. Jiang, X. H.; Wong, B. C.; Lin, M. C.; Zhu, G. H.; Kung, H. F.; Jiang, S. H.; Yang, D.; Lam, S. K. *Oncogene* **2001**, *20*, 8009.
26. Jin, Y.; Chen, Q.; Lu, Z.; Chen, B.; Pan, J. *Cancer Sci.* **2009**, *100*, 2210.
27. Jin, Y.; Chen, Q.; Shi, X.; Lu, Z.; Cheng, C.; Lai, Y.; Zheng, Q.; Pan, J. *Cancer Sci.* **2009**, *100*, 1335.
28. Leuenroth, S. J.; Crews, C. M. *Cancer Res.* **2008**, *68*, 5257.
29. Mak, D. H.; Schober, W. D.; Chen, W.; Konopleva, M.; Cortes, J.; Kantarjian, H. M.; Andreeff, M.; Carter, B. Z. *Mol. Cancer Ther.* **2009**, *8*, 2509.
30. Shi, X.; Jin, Y.; Cheng, C.; Zhang, H.; Zou, W.; Zheng, Q.; Lu, Z.; Chen, Q.; Lai, Y.; Pan, J. *Clin. Cancer Res.* **2009**, *15*, 1686.
31. Li, Z.; Zhou, Z. L.; Miao, Z. H.; Lin, L. P.; Feng, H. J.; Tong, L. J.; Ding, J.; Li, Y. C. *J. Med. Chem.* **2009**, *52*, 5115.
32. Fidler, J. M.; Li, K.; Chung, C.; Wei, K.; Ross, J. A.; Gao, M.; Rosen, G. D. *Mol. Cancer Ther.* **2003**, *2*, 855.
33. Aoyagi, Y.; Hitotsuyanagi, Y.; Hasuda, T.; Matsuyama, S.; Fukaya, H.; Takeya, K.; Aiyama, R.; Matsuzaki, T.; Hashimoto, S. *Bioorg. Med. Chem. Lett.* **2008**, *18*, 2459.
34. Fersht, A. R. *Trends Biochem. Sci.* **1987**, *12*, 301.
35. Sandeep, K.; Ruth, N. *ChemBiochem* **2002**, *3*, 604.
36. Zhang, H.; Trachootham, D.; Lu, W.; Carew, J.; Giles, F. J.; Keating, M. J.; Arlinghaus, R. B.; Huang, P. *Leukemia* **2008**, *22*, 1191.
37. Spahr, H.; Calero, G.; Bushnell, D. A.; Kornberg, R. D. *Proc. Natl. Acad. Sci. U.S.A.* **2009**, *106*, 9185.
38. Ricci, C.; Scappini, B.; Divoky, V.; Gatto, S.; Onida, F.; Verstovsek, S.; Kantarjian, H. M.; Beran, M. *Cancer Res.* **2002**, *62*, 5995.
39. Beran, M.; Pisa, P.; O'Brien, S.; Kurzrock, R.; Siciliano, M.; Cork, A.; Andersson, B. S.; Kohli, V.; Kantarjian, H. *Cancer Res.* **1993**, *53*, 3603.
40. Orsolic, N.; Golemovic, M.; Quintas-Cardama, A.; Scappini, B.; Manshouri, T.; Chandra, J.; Basic, I.; Giles, F.; Kantarjian, H.; Verstovsek, S. *Cancer Sci.* **2006**, *97*, 952.
41. Lu, Z.; Jin, Y.; Qiu, L.; Lai, Y.; Pan, J. *Cancer Lett.* **2009**. PMID:19819619.
42. Pan, J.; Quintas-Cardama, A.; Kantarjian, H. M.; Akin, C.; Manshouri, T.; Lamb, P.; Cortes, J. E.; Tefferi, A.; Giles, F. J.; Verstovsek, S. *Blood* **2007**, *109*, 315.
43. Pan, J.; Quintas-Cardama, A.; Manshouri, T.; Giles, F. J.; Lamb, P.; Tefferi, A.; Cortes, J.; Kantarjian, H.; Verstovsek, S. *Leukemia* **2007**, *21*, 1395.